

An Enhanced Spice and 3D Modelling for Standard Servomotors

PHILIPPE DONDON¹, C.A. BULUCEA²

¹Université de Bordeaux, IPB, Av Dr A. Schweitzer 33405 Talence, FRANCE.

²Faculty of electrical and environment engineering, University of Craiova, ROMANIA

Abstract: Servomotors are widely used and well known by hobbyists for control of small scale radio controlled boats, cars or planes. The control is done using a simple PWM signal modulation, easily compatible with a 2 or 4 channels remote control system. As hobbyists are generally simple users, a light knowledge is generally enough to drive this kind of motor. However, in some electronic applications, we need deeper information on servomotors behaviour. Unfortunately, servo manufacturers never give detailed datasheet and no information is available on various WEB sites. Thus, we present in this paper, a SPICE modelling for hobbyist servomotor. Simulation and practical experimentations are done to validate the modelling. Finally, an additional lively 3D modelling is proposed and a concrete didactical application is described before conclusion.

Key words: Servo motor, Hobbyist, SPICE modelling, 3D modelling, Didactical experience.

Received: August 25, 2020. Revised: February 3, 2021. Accepted: February 25, 2021. Published: March 20, 2021.

1. Introduction

Servomotors are widely used in robotics systems [1], [2] and also by hobbyists in RC (remote controlled) small model cars, planes and boats [3]. However, servo's users often complain about the lack of technical detailed information and servomotor modelling: servos look like a closed "black" box. They are sold without any data sheet or specifications and there is not any reference in academic literature on their internal behavior. Thus, the aim of our work is to propose hereafter an innovating behavior's description (never found before in the hobbyist world) and an original building of a SPICE equivalent modelling of those servomotors.

1.1 Servo motor basics

A classical servomotor for hobbyist [1], [2] is powered under 5V. It consists of a motor with an internal feedback loop to control angle position.

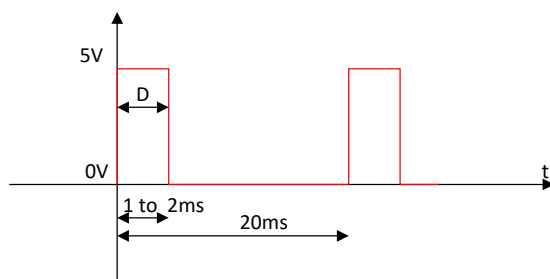


Figure 1: Standard PWM control signal for servo motors.

Servo is driven by a PWM signal at a frequency $f_e=50\text{Hz}$ and a variable pulse width D between 1ms

and 2ms (Cf. figure 1). The angle ϕ changes proportionally to the width of the pulse D from 0° to 180° .

Angular position is internally returned by a potentiometer coupled to the mechanical axis.

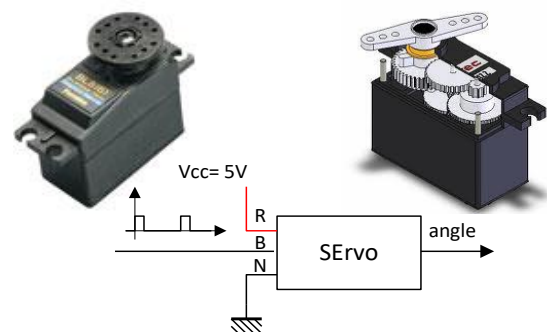


Figure 2: Classical hobbyist servomotor

Main manufacturers [4], [5], [6] gives only a few and basic information as indicated in table 1. In particular, they give the maximum angular speed, (here $60^\circ/0.16\text{s}$) for a standard servo and mechanical torque.

Typical hobbyist servo data		
Volts	Torque	Speed
4.8V	133 oz-in (9.6 kg.cm)	$60^\circ/0.16\text{ sec}$
6.0V	n/a	n/a
Dimensions		Weight
1-9/16 x 13/16 x 1-3/8 in (40 x 20 x 35 mm)		1-9/16 oz (45 g)

Table 1: Basic specification

1.2 Aim and applications of the study

The basic specifications are enough for most of the hobbyist which are simple users and not electronic designers. However, some of us want to use this kind of servomotor for other electronic didactical [7], [8], professional applications or robotic challenges. Then, important data such as static characteristics and dynamic behavior are required to avoid unwanted behaviors. As no modelling “ready and easy to use” exists for this object, we propose here a Spice and 3D modelling of a standard servomotor. This modelling is now used for many didactical student’s projects in second year of study, at Enseirb-Matmeca electronic engineering school: for example, robot design, small car control [9] and also small scale solar tracking system.

2. Modelling approach

In order to build the modelling of the servomotor, we need first to make an easy control of the servo: a DC voltage to PWM converter is placed ahead as indicated in figure 2. It is calibrated to deliver a pulse width between 1 to 2ms proportional to the DC input voltage ($V_{control}$) from 0 to 5V. For that purpose, a simple electronic circuit based on a classical LTC6992 circuit and op amps has been designed.

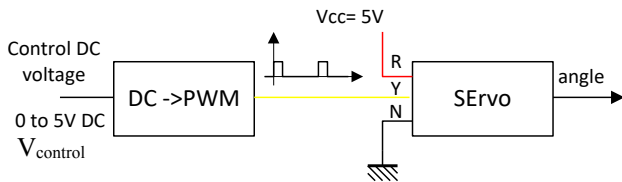


Figure 2: Servo control interface

- R: red wire +5V supply
- Y: yellow wire PWM signal input
- N: ground pin

2.1 Static behavior

With the schematic of figure 2, rotation angle ϕ becomes proportional to the input control DC voltage $V_{control}$:

From a static point of view, the equivalent SPICE model is a simple proportional angle-voltage factor k :

$$k = 180^\circ/5V \text{ (in } ^\circ/V) \text{ or } k = \pi/5V \text{ (in rad /V)}.$$

2.2 Transient behavior

The reaction of servomotor when applying a voltage ramp slow enough, on DC input is shown in figure 3. Rotation angle follows the evolution of input voltage with a small constant delay (cf. section 3).

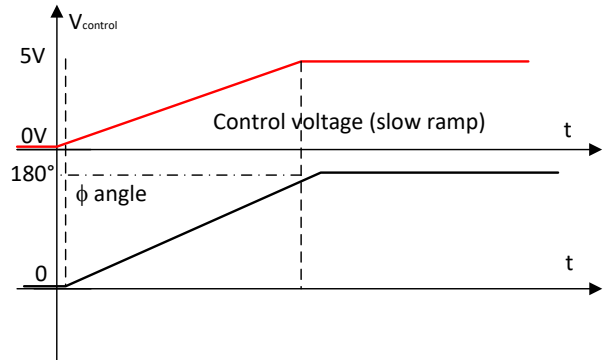


Figure 3: Response to a slow ramp voltage input

Figure 4 shows the reaction of servomotor when applying a pulse voltage on input: due to the intrinsic limit of velocity given by the manufacturer (here $60^\circ/0,15s$), response looks like a ramp; angle will change with a limited speed.

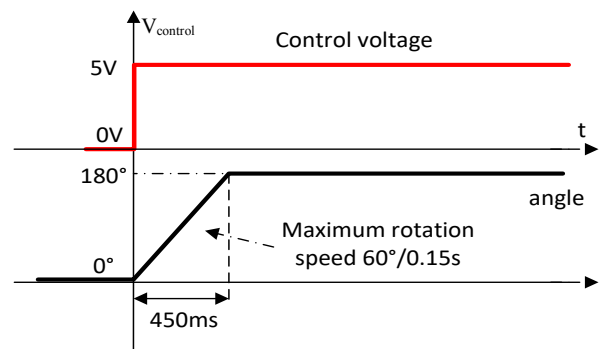


Figure 4: Response to an input pulse voltage

From these two transient observations, we deduced that a “speed limitation” or “saturation” block must be included in the Spice modelling.

2.3 Mechanical dynamic behavior

From a dynamical point of view, the behavior of the servo can be analyzed by looking at each component (cf figure 5):

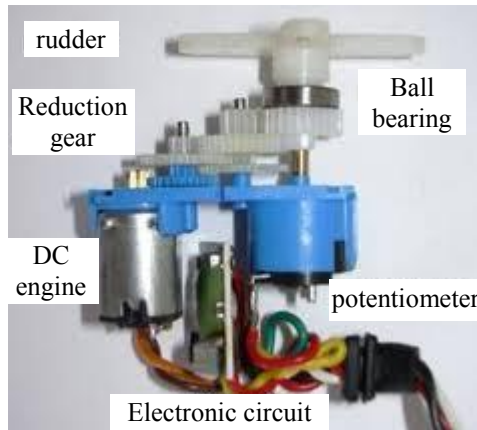


Figure 5: exploded view of a servo

a) DC motor engine

A DC motor (cf. figure 6) is classically described by a set of two coupled electrical and mechanical equations [10], [11]:

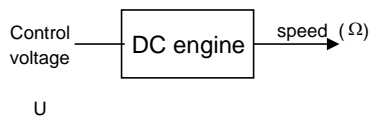


Figure 6: DC motor

$$U = E + R.I + L.dI/dt \quad (1)$$

Where:

- U is the voltage applied to the motor,
- E is the back electromotive force $E = k\Phi\Omega = K_E \cdot \Omega$,
- R is inductor resistor,
- I is the current across the motor,
- Ω is rotation speed (rad/s),

And:

$$C_m = J.d\Omega/dt + C_r + C_f ; C_m = P_m/\Omega = K_C.I \quad (2)$$

Where:

- C_m is the motor torque,
- J is the inertial moment,
- P_m is the mechanical power,
- C_r is the resistant torque.
- C_f is the friction torque

In practice, $K = K_c \approx K_E$ and the servo load is generally very low (see application in section 7.) . The transfer function $H_M(p)$ “speed vs. applied control DC voltage” can be written:

$$H_M(p) = \Omega/U = 1/K.[1/(1 + p.R.J/K^2 + p^2.L.J/K^2)] \quad (3)$$

With hobbyist servomotor, we can assume that damping factor is greater than 1. The transfer function

becomes a simple first order function with a dominant mechanical time constant:

$$H_M(p) = \Omega/U = 1/(1 + p.R.J/K^2) \quad (4)$$

b) The reduction gear

It is a simple train of gears which lowers the speed of the propeller shaft depending on the relative number of cogs.

c) The angle sensor

In standard servomotors, it is a simple rotating potentiometer coupled to the shaft. The output voltage is proportional to the angle.

From this basic description, we can propose a first modelling corresponding to schematic in figure 2.

3. Servomotor basic SPICE modelling

The servomotor (controlled in position) can thus be represented by the following blocks (from Analog Behavior Modelling “ABM”, SPICE/ORCAD library):

- a set up voltage DC value $V_{control}$ (corresponding to a set up a given angle value ϕ_{ref}),
- a coefficient $k=0.62$, representing the ratio between $V_{control}$ and ϕ_{ref} angle reference value (in rad) (cf. § 2.1),
- a comparator «set up value /returned angle value »,
- a first order transfer function:

$$\Omega(p)/U(p) = 1/(1 + \tau.p)$$

It represents the response speed vs. control voltage of the motor according to equation (4). The cutoff frequency value (here 15Hz, i.e. $\tau = 0.01s$) was previously obtained by experimental transfer function identification,

- an additional function “saturation of rotation speed” (cf. § 2.2), which represents the maximum possible rotation velocity of the servo: When the speed is under the limit this function is “transparent”, when above, the limit is imposed by this function,
- a constant factor ($G=10$), which represents the reduction gear (it was obtained by experimental characterization),
- a pure integrator function $\phi(p)/\Omega(p) = 1/p$ which represents the conversion from speed Ω to angular position ϕ (in rd).

It leads to the following schematic in figure 7:

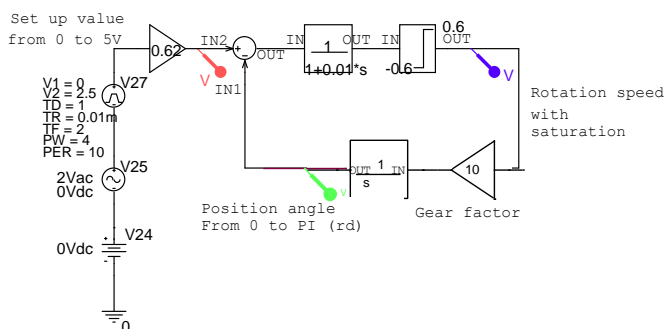


Figure 7: Basic SPICE modelling

Figure 8 shows a transient response of this modelling submitted to a pulsed input voltage; When the set up voltage value change extremely quickly (positive edge), the servomotor turns and the angle increase linearly at its maximum speed (i.e around $60^\circ/160\text{ms}$). When the set up value V_{control} is constant, there is no static error thanks to the natural integration in the loop (speed \rightarrow position). When the set up value changes slowly (negative edge) the servo motor follows with a permanent following error.

Red trace: set up control angle value ϕ_{ref} (rd)
 Green trace: angular rotation ϕ (rd)
 Blue trace: rotation speed Ω
 (horizontal time scale 0 to 10 s, vertical scale in rd)

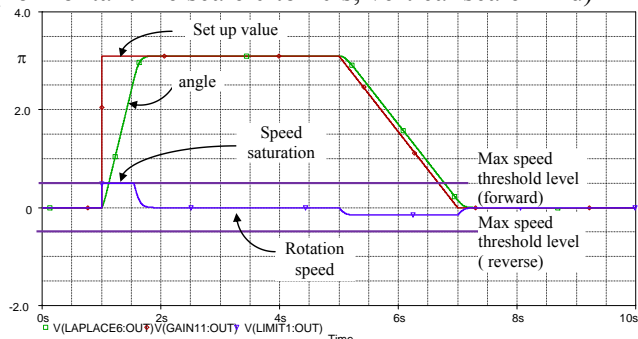


Figure 8: Simulated transient response

We must notice that:

- a) The saturation block is well simulated in transient mode but not in AC analysis. Thus, frequency simulation will not be perfectly correct.
- b) This first SPICE modelling is suitable for variations of control signal under $F_e=50\text{Hz}$. When upper, and because of PWM signal characteristics, the duty cycle is updated each 20ms, which equivalent to a sampling system.

Thus, it is necessary to improve and complete this basic modelling as indicated in paragraph 3.

4. Improved servomotor modelling

In most of application, servomotors are remotely controlled by R/C model driver or pilot by two joysticks, through a two or four channels HF R/C emitter receiver. The movement of the joystick is obviously slow compared to the electronic time constant, because it is moved by the human hand. In that case, the first modelling is enough for that purpose.

However, one of specificities of hobbyist servomotors compared to other is the PWM signal control. It is not actually an advantage for electronic designer because it introduces some unwanted behaviors. Indeed, the pulse width is updated each 20ms: It is like if the control voltage V_{control} (cf. figure 2) was sampled at a frequency $F_e = 50\text{Hz}$.

If the control signal V_{control} varies at a frequency lower than 50Hz (purple trace on figure 9), pulse width of PWM signal (black curve) is well proportional to the instantaneous V_{control} value. So, sampling does not affect the servo and it works correctly. If the frequency of control signal is higher than 50Hz (green trace on figure 10), there is an under sampling; the apparent control voltage (red curve) takes “random” values at each sampling interval (i.e. 20ms) (red dots on figure 10) and has obviously no relation with the initial green curve: in this situation, the servo does not work anymore correctly.

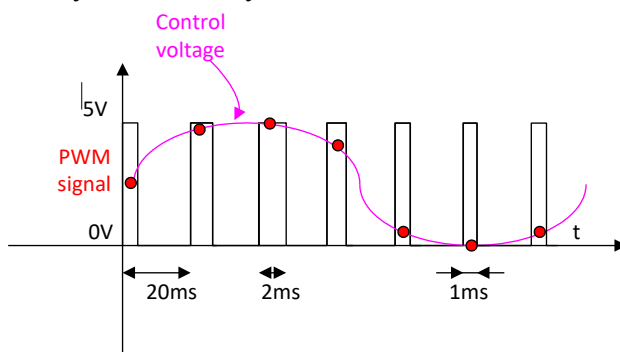


Figure 9: Representation of correct sampled control signal.

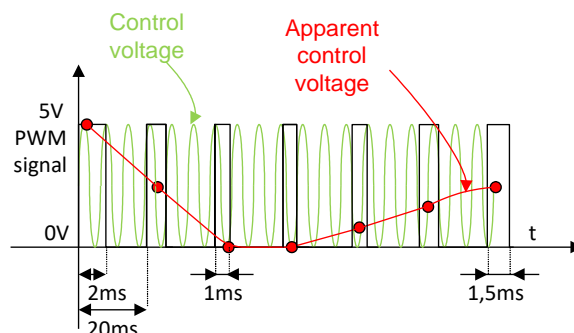


Figure 10: Representation of under sampled control signal

Thus, we need a more improved modelling for our non-hobbyist applications, which takes into account the impact of PWM signal.

In order to represent the sampling effect, a voltage controlled switch “VC_Switch” Spice component and C1 (holding capacitor) are added to the previous modelling as indicated on figure 11.

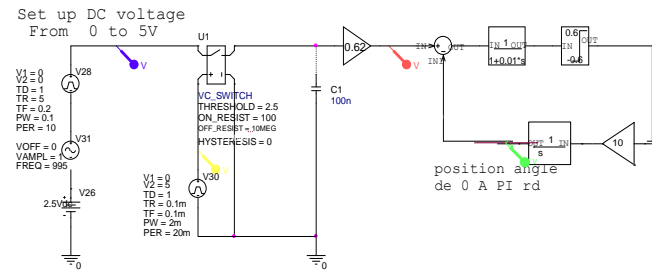


Figure 11: Improved SPICE servomotor modelling

Simulation in figure 12 shows the transient response on this new modelling. Zoom shows the step on control value due to the sampling. During the slow positive ramp, the servomotor follows correctly from 0° to 180° with a constant following error. During the hard negative slope, the servomotor turns at its maximum speed (# 180°/450ms).

Red trace: sampled set up control angle value (0 to π)
 Green trace: rotation angle ϕ (in rad)
 Vertical scale: 1V \Leftrightarrow 1 rad
 Horizontal scale: time 0 to 7s

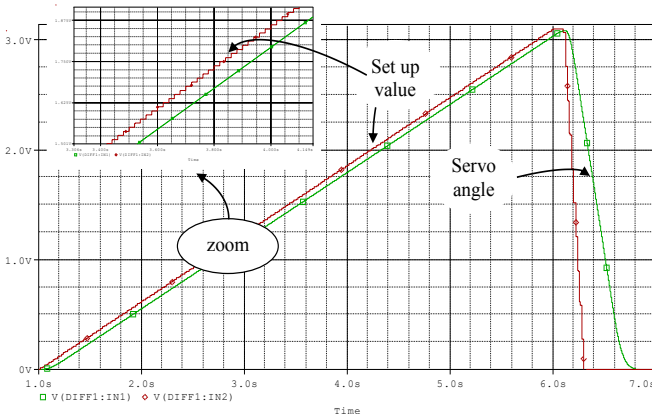


Figure 12: Response to a ramp from 0 to 5V (rotation from 0° to 180°)

Figure 13 shows the response to a slow sinus variation of the set up voltage value (1Hz, 1.5V offset, peak value 2V). The output angle follows the input at the right frequency but with a limited amplitude and limited slope because of the maximum rotation speed. We can say that this phenomenon is equivalent to the slew rate of an OP amp. (Here, maximum input slope

@ t=0 sinus $dV/dt = 12.56V/s$ (maximum output slope 3.14 rd/450ms, i.e. 6.9 rad/s)

Red trace: sampled set up control angle value
 Green trace: rotation angle (in rad)
 Horizontal scale: time 1 to 5s

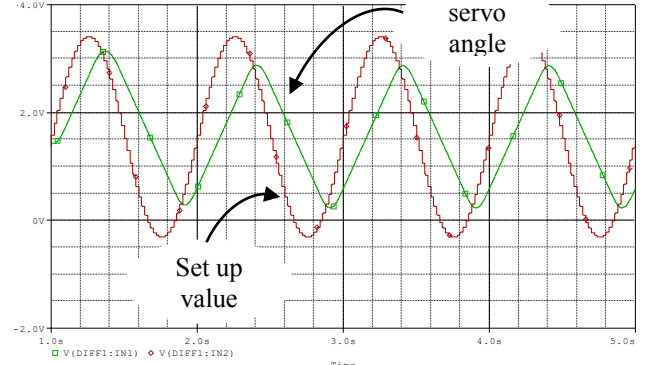


Figure 13: Response to a slow sine wave control signal

When the control signal varies at a frequency F_{setup} higher than 50Hz (PWM frequency), the under sampling phenomenon appears (cf. figure 10).

Rotation angle ϕ is then affected. Oscillation may occur at a frequency mixture $F = N' \cdot F_{setup} \pm N \cdot F_e$ between harmonic of F_{setup} (N') and harmonic of PWM frequency F_e (N),

Thus, when applying a sine wave on the control voltage input at higher frequency than 50Hz, the servomotor will oscillate incorrectly at composite frequencies that are into the servo bandwidth.

For example, Figure 14 shows the response of the servo when a sine wave at 66Hz and peak voltage of 3V (i.e. hoped angle rotation 108°) is applied to the input control voltage. At this frequency, effects of sampling and speed limitation are combined.

Green trace: rotation angle ϕ (in rad)
 Vertical scale: 1V \Leftrightarrow 1 rad
 Horizontal scale: time 0 to 5s

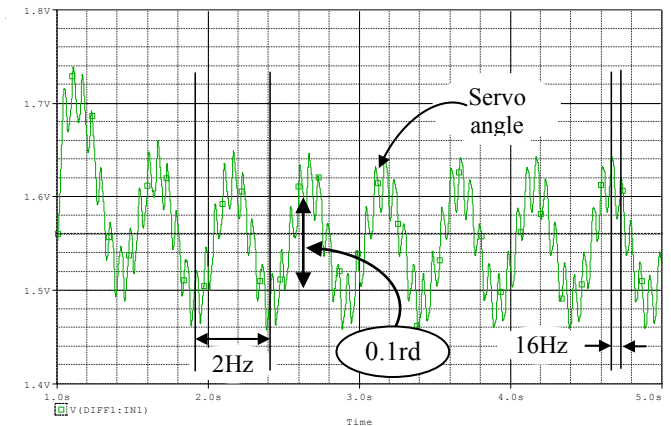


Figure 14: Response to a “fast” sine wave applied on Vcontrol signal ($f = 66$ Hz)

In this situation, servomotor does not move correctly: here, we observe composite movements with oscillations at 2Hz (=4*50Hz-3*66Hz) and 16Hz (=66Hz-50Hz). The average peak to peak value of angle rotation is 0.1rad or 5.7° (instead of the 108° hoped).

As said before, and because of the behavior of SPICE blocks, an AC frequency spice analysis is not possible. Thus, to get an overview over a wide frequency range, a set of transient analysis at different given frequency must be performed.

5. Results checking and comments

5.1 experiments

Practical experimentation has been done with two medium servomotors from two different companies.

An Agilent function generator has been used to generate the input control signal. A simple interface analogue circuit to convert DC voltage into PWM signal has been built including LTC6992 (Voltage-Controlled Pulse Width Modulator), a “rail to rail” Op Amp LM6482 and some other basic components.

By opening very carefully the servomotor box and placing a probe on the cursor pin of the potentiometer (see figure 5), it is possible to get an image of servomotor movement. Response are observed on oscilloscope.

Three tests were performed:

1) Step stimuli from 0 to 5V applied at the control voltage input: according to figure 4, servo rotates at its maximum speed: a voltage ramp from 0 to 5V is observed on potentiometer output and time to go from 0° to 180° is 450ms which is coherent with figure 12, negative slope on green curve.

2) Slow triangle stimuli from 0 to 5V applied at the control voltage input: Waveform on potentiometer output reproduce correctly the triangle, with a short time delay of around 0.1s which corresponds to value obtained on figure 12. The servo rotates correctly over the full range from 0 to 180° and back to 0°.

3) Sinus wave stimuli 3V peak, 66Hz: Servo oscillates at 2Hz as predicted by simulation. However, the 16Hz contribution is not really visible and measurable.

We obviously could have studied more finely accuracy of these results. However, matching between simulation and experiments are enough satisfying at the first order for our applications.

Unfortunately, we cannot compare with other studies because of the lack of academic information on hobbyist servo, as told in section 1.

5.2 Comments

From these observations and results, we can now conclude about some of the missing specifications on servomotors: the maximum frequency range in which the classical servo can operate correctly. To avoid unwanted oscillations, variations of the set up voltage value must be theoretically slower than $F_e/2$, i.e. 25Hz and, in practice, lower than $F_e/10$ for proper operation, (i.e. angular position follows correctly the set up control value). Thus, such servos are suitable for extremely slow movements [17]. Sometimes, it is possible to find commercial RC model cars (for example Nikko) [9] with “open loop steering wheel servo”. In that case, potentiometer sensor is directly accessible for users to design a voltage feedback loop circuit, avoiding DC to PWM converter. Then, it is possible to enhance the speed performance or the servo compared to the previous described situation.

5.3 Modelling limits, pro and cons

Main aim of this work is to offer to hobbyists who generally use servo as a black box and who are not highly familiar with electronics, a simulation model for R/C servomotors.

Firstly, this modelling could appear a little bit complex for those who do not have basic knowledge in electronic. Thus it requires for users to acquire first some electronic skills.

Secondly, this Spice modelling is not a parametric model. It dedicated to small hobbyist servo used for R/C cars, plane and boats. It might be not valid for high power or industrial servo.

However, for those people who have electronic knowledge, this modelling is easy to use. As it is a looped system, a particular attention must be paid when including this model in a bigger schematic as described in section 7. In this example, there are two nested loops (servo motor and global feedback). Thus, typical convergence problem could occur during simulation.

6. Additional 3D modelling

In order to get a complementary and “live view” of modelling simulation results, a 3D modelling can be shortly built using Virtual Reality Modelling Language [12], [13].

6.1 VRML short overview

The Virtual Reality Modelling Language (VRML) was born in 1995 [12], [13], [14]. It aims to create and to animate any graphic objects. It was initially used for gaming and also for didactical applications. The graphical animation module of the well-known MATLAB software is based on VRML. It is “rustic” freeware and it requires only an internet navigator such as Firefox and a “plug in” like “cosmoplayer” or orbisnap viewer to play the animations. Creation and description of 3D objects can be done using a simple text editor. Movement and animation can be programmed either in VRML or in JavaScript [15]. Here, we can use VRML to visualize the servomotor sweep in 3D image, to get a more realistic understanding of system behavior than the previous 2D curves given in figure 12 for example.

6.2 VRML drawing and data exportation from SPICE to VRML file

As we do not need too much esthetical and sophisticated geometrical drawing, a simple and symbolic view of the servo based on box and cylinder basics shapes has been drawn in Cartesian coordinates and saved into a *.wml file (figure 15). The biggest interest is not the drawing itself but more surely the movement visualization in 3D.

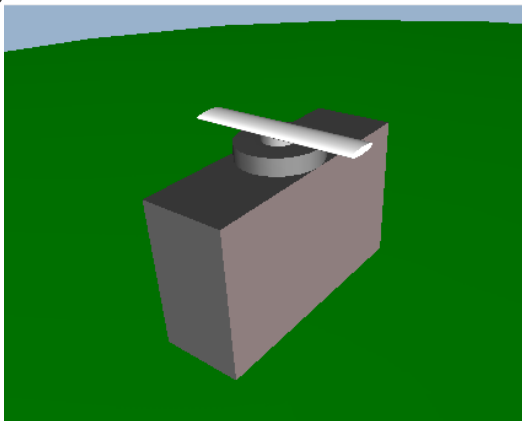


Figure 15: VRML 3D modelling of servomotor

This can be done by exporting data from previous SPICE runs and including them after file conversion into the VRML description file. Indeed, the spice transient simulation result are available as graphical curves but also as output file *.dat containing a table of values: for transient simulation of figure 12, we get a set of data organized as follows:

- Time instant t_i , from 0 to T_{max} (s), with a time step defined automatically by Spice,
- Setup control angle value ϕ_{ref} , (with $1V \Leftrightarrow 1rd$),
- Angular servo position ϕ (with $1V \Leftrightarrow 1rd$),

Since VRML works in normalized time and with a greater time step than Spice, some adaptations and conversions must be done, before exporting Spice data to a VRML file.

Figure 16 summarizes the main steps of the data conversion process, to convert data from Spice simulation into VRML data.

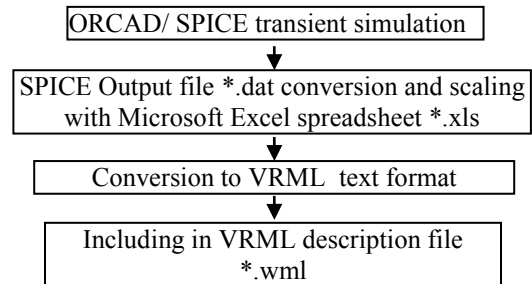


Figure 16: SPICE to VRML data conversion process

5.3 Running animation

in VRML language, the movements of the object are described as a combination of translation and rotation. in the chosen Cartesian coordinates Some line of codes must be added in the description file *.wrl. Translations are defined into a kind of table named “keyvalue”: For each normalized time instant t_i/t_{max} , the instantaneous corresponding 3D position x_i, y_i, z_i is given in a table with the syntax indicated below.

```

DEF course PositionInterpolator {
    key [t0/tmax, ..., ti/tmax, ..., 1]
    keyValue [ x0 y0 z0, ..., xi yi zi, ..., xn yn zn]}
    
```

Rotations, which are more suitable for us in this example, are defined as follows: for each normalized time instant t_i/t_{max} , the instantaneous corresponding rotation axis x, y, z and rotation angle α (in rd) are specified in a table according to the syntax given below.

```

DEF rotcapt OrientationInterpolator {
    key [t0/tmax, ..., ti/Tmax, ..., 1]
    keyValue [x y z α0, ..., xi yi zi αi, ..., xn yn zn αn]}
    
```

For example, a rotation of $+\pi$ around the Y axis will be specified with $x_i = 0, y_i = 1, z_i = 0, \alpha_i = 3.14$.

Then, the animation can be played with one time or be looped to replay the animation permanently. The animation cycle time duration T_{sweep} (or *cycleInterval*) in second, of the animation is specified as follows:

```

DEF temps TimeSensor {
    
```

*cycleInterval 30
 loop TRUE}*

7. Example of application

The SPICE and 3D modelling of the servomotor presented before, has been used within the framework of student's project in second year of study at Enseirb-Matmecca electronic school [16], [17], [18].

A small scale light tracking system was studied and designed by the students. The aim was to follow and to point towards a spot light whatever its position into a geometric horizontal plan, like a human could do with his eyes by turning his head. The synoptic is given in figure 17.

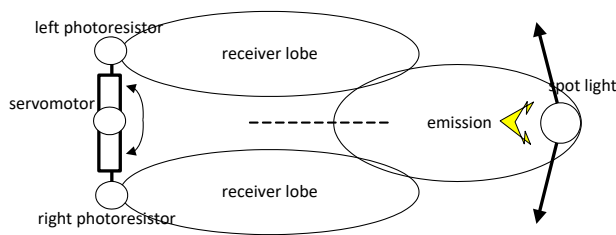


Figure 17: Light tracking system principle

The system works as follows: two light sensors LDR1 and LDR2 (LDR: visible light spectrum photo resistors), located on left and right side of a mechanical arm receive the light. When the system is well aligned in spotlight direction, the received left and right lights flux L_1 and L_2 are equal. When it is not, one of the two LDR receives more flux than the other, and feedback loop moves the servo motor into the right direction to cancel the voltage difference V_{diff} "left minus right" signals (Cf. figure 17 and 18).

7.1 Electronic design

The experimental electronic circuit was built as follows: The two matched LDR sensors (VT90N2) are included in a Wheatstone bridge. Output signals are amplified and subtracted using rail to rail OP amps LMC6482. Difference is applied to a PID corrector. The resulting DC voltage value is converted linearly (i.e. pulse width proportional to DC voltage value) into a PWM signal, to control a classical Futaba servomotor (cf. figure 18).

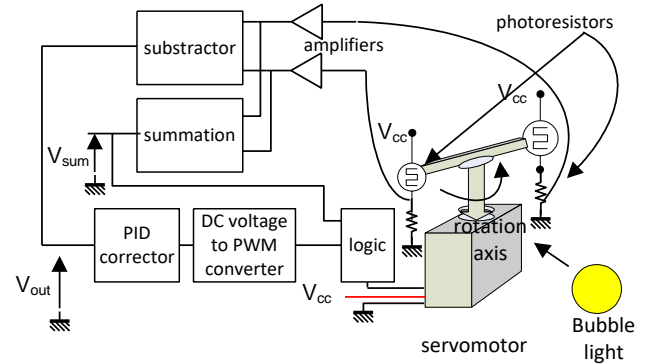


Figure 18: Bubble light tracking system

7.2 Modelling

The system has been modelled as indicated in following figure 19 with the following hypothesis:

- α_{ref} is the main input of the feed-back loop system and correspond to the bubble light azimuth position (limited to 0° to 180° to be compatible with servo range),
- L_1, L_2 are the received light (in Lux) by the two left and right photo resistors,
- α is the angular position returned by the servo motor,
- α_e is the error angle,
- "I" is the bubble light intensity,
- V_{diff} is the voltage difference coming from sensors,
- D is possible optical disturbances on the light path between bubble light and sensors, (object passing over...)

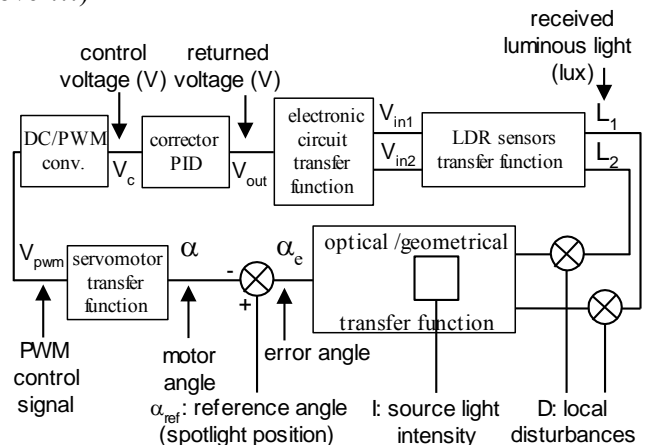


Figure 19: Tracking modelling block diagram

After mathematical, geometrical and optical understanding, calculus and/or identification, a global complex Spice modelling was established. Since the motion of bubble light is very slow (moved by human hand), the first modelling of the servo as defined in figure 7, was used and included in the global modelling (cf. figure 20).

A more detailed description of each block is available in a previous publication [19].

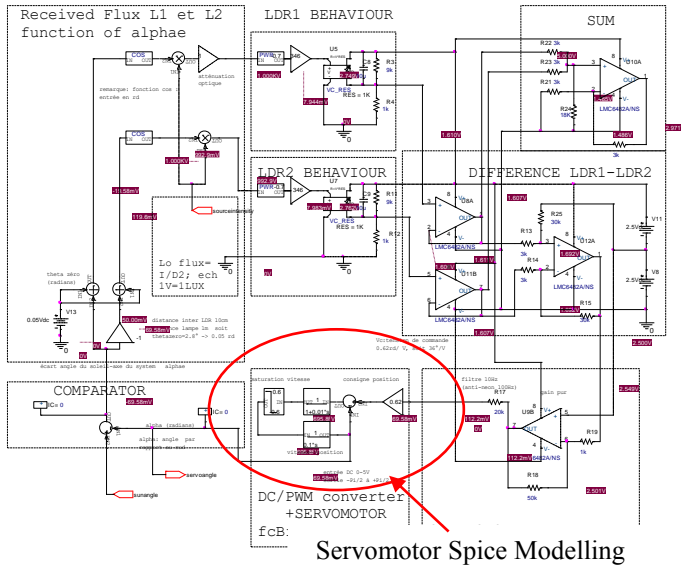


Figure 20: Global Spice modelling

A simulation corresponding to a circular horizontal sweep of the bubble light from left to right was performed. Once validated, transient results data were exported to VRML file to visualize in 3D, the movement of the system.

Figure 21 and 22 show two snapshots during the sweep of bubble light, in orbisnap VRML viewer. The two left and right sensors track correctly the movement and are aligned with the light.

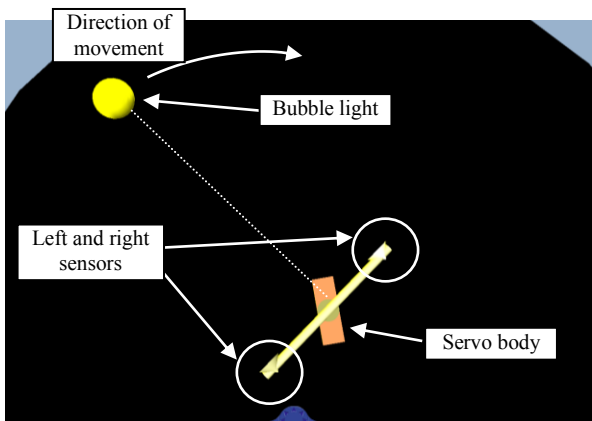


Figure 21: Light tracking 3D animated modelling (top view)

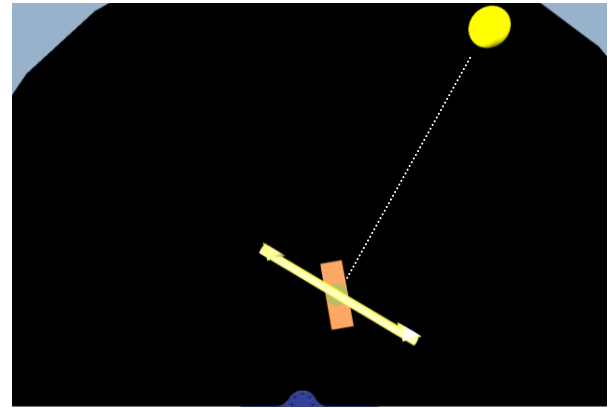


Figure 22: Light tracking 3 D animation

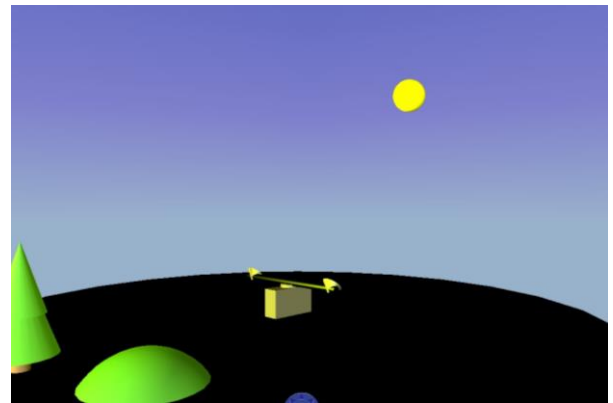


Figure 23: side view

8. Conclusion

An “easy to use” modelling of standard hobbyist servomotor have been built and presented. This modelling is suitable for standard servo and fit the needs of Hobbyists as well as the one’s of electronic designers. For micro and large servomotors series, some adaptations must be done (torque and time constants). A comparison between practical behaviour and simulation showed a correct matching between modelling and servomotor behaviour. In addition, a 3D animated model has been developed. Finally, an example of a complex circuit including the modelling has been presented to highlight interest of this servomotor Spice and 3D modelling.

References:

- [1] Futaba web site: <http://www.futaba-rc.com/>
- [2] Hitec web site: <http://hitecrcd.com/>
- [3] Parallax web site: <http://parallax.com/>

- [4] V. Vaillant, J. Pastre, Ph. Dondon, Alternating approach of student's project oriented to modular design in high engineering electronic school : example of autonomous small-scale electric car design with embedded navigation module, WSEAS Trans on Servomotor Spice Modelling Left and right sensors Servo body Bubble light Direction of movement advances in engineering education Vol. 15, pp. 34-43, 2018 E-ISSN: 1790-1979 / 2224-3410
- [5] Web site linxmotion: <http://www.linxmotion.com/c-1-products.aspx>
- [6] Web site fribotte: http://fribotte.free.fr/bdtech/pic/pic_et_servo.html
- [7] Ph. Dondon, J.Micouleau, G. Leroyer, Introducing embedded system concept through a multi thematic funny hexapod robot design project, WSEAS EDUTE '08 26-28 octobre 2008 Corfou (Grèce)
- [8] Ph. Dondon, L. Miron, Modelling and design of a small scale solar tracking system; Application to a greenhouse model, int. conference EED'14 WSEAS 26-28 june 2014 Brasov Roumania.
- [9] Ph. Dondon, A. Dutrey, J. B. Bourlier, A. Sivert, Designing a COTS electronic system for trajectory correction of a Radio controlled model electrical car, WSEAS trans. on power systems, Vol. 12, pp. 183-195 2017 E-ISSN: 2224-350X
- [10] Fr. Bernot « Chapitre 2-1 : Machines à courant continu » Document n° DS30060, FranceCol Technology.
- [11] G. Pinson « Physique Appliquée, chapitre C32 » <http://www.syscope.net/elec/C32.pdf>
- [12] M. Divjak, D. Ko Visual and audio communication between visitors of virtual worlds WSEAS multiconference, Tenerife 2001
- [13] S. Duta, M. Mitrea, F. Preteux « VRML versus Inventor: bridge the gap » WSEAS Transactions on Communications 3, 3 (2004) 884-890
- [14] S. Marnier « VRML course », web site: <http://grandm.free.fr/apprend/vrml/00index.html>
- [15] Ph. Dondon, M. Marthiens Dagorette, J.M Micouleau, A.Bulucea Exploration of Virtual Reality Modelling Language world and its didactical applications. WSEAS Trans on Advances in Enginneering Education Vol.11, p.32-44, 2014 ISSN: 2224-3410
- [16] F. Berthier, A. Berge. “asservissement de position par faisceau infrarouge” Internship report Enseirb-Matmeca 2012
- [17] F. Konrad, A. Labarthe “traqueur de lumière” Internship report Enseirb-Matmeca 2012
- [18] S. Jacques, Z. Ren, S. Bissey, A. Schellmanns, N. Batut, T. Jacques, E. Pluvinet, An innovative Solar Production Simulator to better teach the foundations of photovoltaic energy to students, WSEAS Trans on advances in engineering education Vol 11, pp.11-20 2014 ISSN: 2224-3410
- [19] Ph. Dondon, L. Miron, Modelling and design of a small scale solar tracking system; Application to a green house model, WSEAS transactions on circuits and systems Vol. 13, pp. 452-463 2014 E-ISSN: 2224-266X
- [20] M. C. Brady, A Low Cost Desktop Robot and Tele-presence Device for Interactive Speech Research, INTERSPEECH 2016: Show & Tell, sept 8-12 2016, San Francisco, USA
- [21] Shen X. et al, Teleoperation of On-Road Vehicles via Immersive Telepresence Using Off-the-shelf Components. In: Menegatti E.,

Creative Commons Attribution License 4.0 (Attribution 4.0 International, CC BY 4.0)

This article is published under the terms of the Creative Commons Attribution License 4.0
https://creativecommons.org/licenses/by/4.0/deed.en_US